R&D Studies on the influence of the addition of percentage quantities of CH_4 to pure xenon

E.D.C. Freitas,[*] M.R. Jorge, L.M.P. Fernandes and C.M.B. Monteiro

Departamento de Física, Universidade de Coimbra
Rua Larga, 3004-516 Coimbra, Portugal

E-mail: elisabete@gian.fis.uc.pt

ABSTRACT: In the present work, relative measurements have been performed for the EL yields of xenon and xenon-mixtures in a uniform electric field driftless GPSC. The operational parameters of the detector, including amplitude, energy resolution and drift velocity, were measured as a function of the reduced electric field in the scintillation region. For an E/p of 3.5 V/cm/torr, the energy resolution has values of 8.1%, 8.3% and 12% for pure xenon, 99.5%Xe + 0.5%CH_4 and 99.0%Xe + 1.0%CH_4, respectively. The scintillation amplification parameter for pure xenon was used as reference to obtain the relative EL yields of 68 photons/kV for xenon with 0.5% of CH_4, 38 photons/kV for 1% of CH_4 and 15 photons/kV for 2.2% of CH_4. This reduction in EL has to be taken into account if the addition of CH_4 to xenon is to be considered.

KEYWORDS: Electroluminescence; molecular additives; xenon.

May, 2014

[*] Corresponding author.

Contents

1. Experimental Setup

The detector is a driftless GPSC, with a 10-cm in diameter and 2.5-cm deep scintillation region, filled with xenon or xenon-CH_4 mixtures at pressures close to 1 atmosphere, continuously purified through SAES St-707 getters. The upper part of the detector body is made of Macor, which insulates the 8-mm diameter Kapton radiation window from its stainless steel holder. The Kapton, the stainless steel and the Macor are epoxied to each other. The Kapton window is aluminised on the inner side to ensure electrical conductivity. The lower part of the detector is built from stainless steel and connected to the gas circulation system. The bottom of the detector is a Macor disc epoxied to a 51-mm diameter PMT and to the detector wall. A chromium grid of ~100-μm in line width and 1000-μm spacing is vacuum-deposited onto the PMT quartz window and connected to the photocathode pin through a continuous chromium film deposited on the side surface. The upper and lower parts of the detector are made vacuum-tight by compression of an indium gasket. The Kapton window and holder are kept at negative high voltage, while the chromium grid and the PMT photocathode are kept at 0V. The window holder and the upper Macor piece were designed to ensure a uniform electric field in the scintillation region [1].

The electric field points towards the window, so that electrons travel in the opposite direction, towards the grid. The Macor electrically insulates the window from the remaining detector body.

The photosensor, a photomultiplier tube (PMT) with quartz window for VUV scintillation light detection, has advantages such as suitable detection area and quantum efficiency, low dark current and high gain (10^5-10^6).

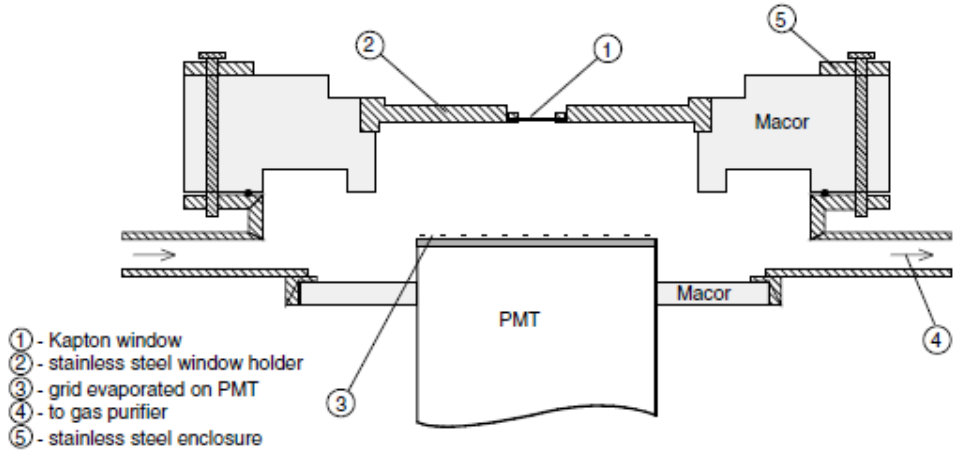

Figure 1: Scheme of the driftless GPSC used in this work, already used in [1].

The charge signal from the PMT was pre-amplified and subsequently formatted with a linear amplifier, with integration/differentiation constants of 5 μs. The formatted pulses were collected with a multichannel analyser (MCA) of 1024 channels.

The preamplifier is a Canberra model 2004, and for the present tests a sensitivity of 9 mV/MeV was chosen. The linear amplifier, an HP 5582 A, has variable independent gain and formatting constants (differentiation and integration). The amplifier is connected to the MCA.

Gas system

There are two main gas systems associated to the detector, namely a purifying system with getters and a system to add molecular impurities, presented in figure 2.

The first system was used to purify and circulate the gas (see figure 2, from valve T1, including T2, T3, to valve T4, in black) and another one to introduce the molecular impurities into the detector (from valve T4 to the CH_4 bottle). SAES St 707 getters were used throughout the whole experimental work to purify the gas by convection. During the experiment, getters were maintained at temperatures in the range of 100°C to 150°C.

With different independent volumes, it was possible to control the quantity of CH_4 that was introduced in the detector and, this way, we could have different percentages of xenon and CH_4 inside the detector volume.

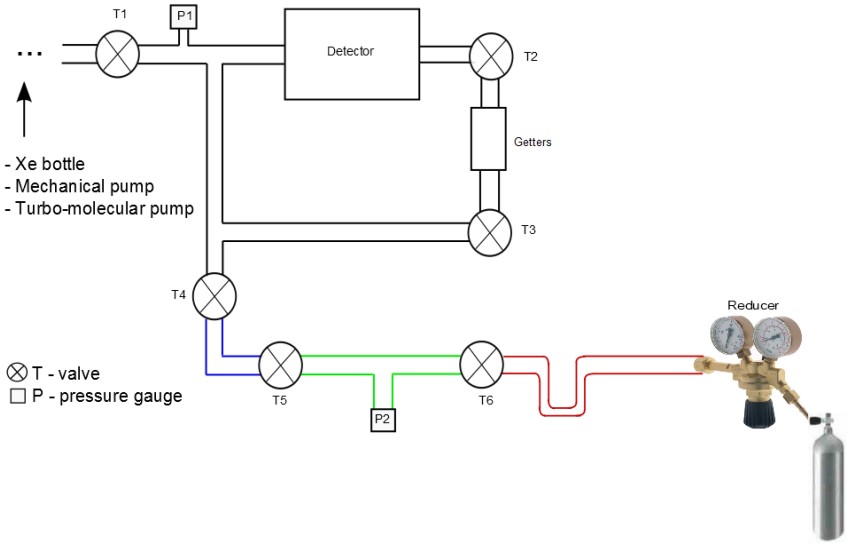

Figure 2: Scheme of both gas systems connected to the detector.

The U tube presented in figure 2 allows for the condensation of the methane gas with the help of liquid nitrogen. This is useful when we want to collect the methane gas.

Small quantities of methane were added to xenon in the detector, through the molecular impurities gas system. To have mixtures of (100-x)% Xe + x % CH_4 we calculated the ratio of the different volumes in our experimental system, in order to know the percentage of CH_4 , using the following equation:

$$P_i V_i = P_f V_f$$

2. Experimental Results

In this work, we performed electroluminescence (EL) measurements, such as amplitude and energy resolution of secondary scintillation pulses that result from the interaction of 5.9 keV X-rays from a ^{55}Fe radioactive source.

A thin chromium film was placed between the radioactive source and the detector radiation window to absorb efficiently the most part of the 6.4 keV X-rays (Mn K_β line), which are emitted by the ^{55}Fe together with the 5.9 keV X-rays (Mn K_α line).

In the case of pure xenon, we considered different temperatures for the getters, from 100 to 150^{o}C and pressures of about 800 torr.

2.1 Pure xenon

Figure 3 shows a typical pulse-height distribution obtained with pure xenon for 5.9 keV X-rays.

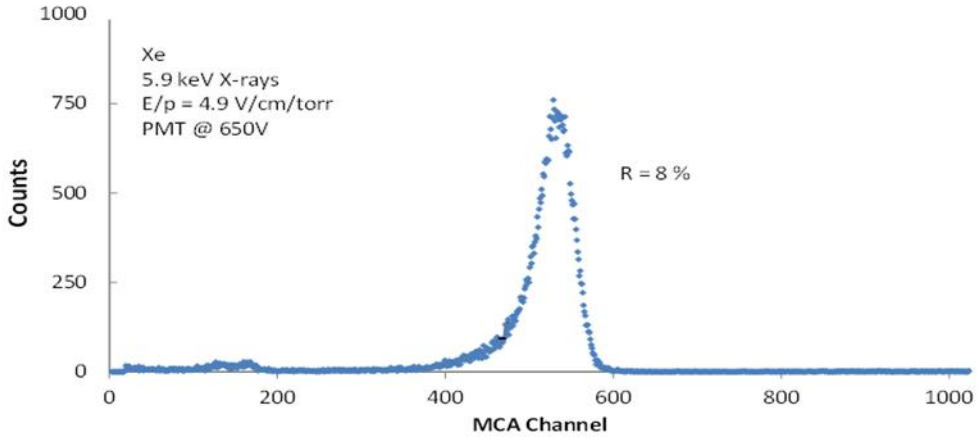

Figure 3: Pulse-height distribution for 5.9 keV X-rays absorbed in the xenon driftless GPSC. The PMT was biased at 650 V, the reduced electric field was 4.9 V/cm/torr and formatting constants were 5 μs.

Figure 4 presents the relative amplitude and energy resolution as a function of E/p of the driftless GPSC filled with xenon at a pressure of 798 torr for shaping constants of 5 μs, while the temperature of the getters was set to 150°C. For 5 μs the collected signal corresponds to the total amount of EL produced in the whole scintillation region.

From the amplitude as a function of E/p, the scintillation threshold can be deduced, that is, the E/p value corresponding to the intersection of the straight line fit to the amplitudes (figure 4) with the E/p scintillation axis, i.e., the value of E/p where the EL starts to be produced. This value was found to be ~1.0 V/cm/torr for pure xenon, which is in agreement with the values reported in the literature [2].

The number of photons produced per primary electron that reach the scintillation region is proportional to the E/p_{scint} [3]. Therefore, for the same PMT bias voltage, the higher the E/p, the higher the amount of secondary scintillation and, consequently, the larger the signal amplitude detected by the PMT. In the scintillation region, the relative amplitude increases linearly between the excitation and the ionization thresholds, for long shaping constants.

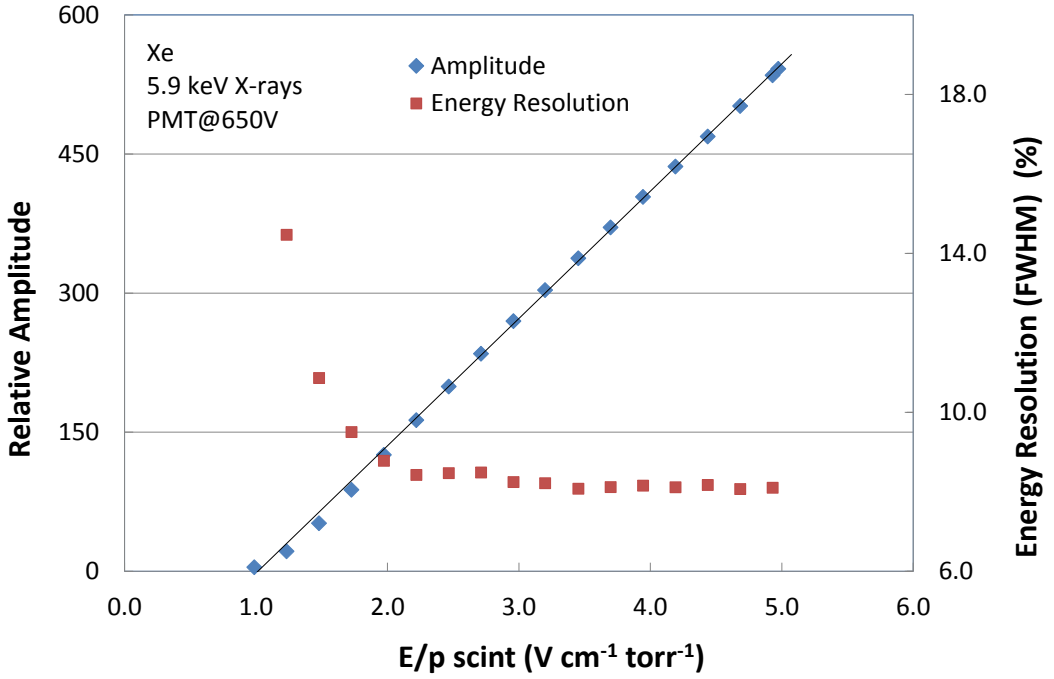

Figure 4: Relative amplitude and energy resolution as a function of reduced electric field, E/p, for pure xenon with getters operating at 100°C and for 5 μs shaping constants. A PMT bias voltage of 650 V was used and the gas pressure was 804 torr.

Also for 5 μs, the energy resolution decreases rapidly as E/p increases in the scintillation region, especially after reaching the excitation threshold. The energy resolution stabilizes after ~3.0V/cm/torr. This is due to the strong increase in the quantity of EL produced in the scintillation region. Since primary electrons gain more energy from the electric field, they produce quantity higher amount of scintillation.

From a certain value of E/p on and until the onset of ionization, the amount of EL is high enough for the statistical fluctuations inherent to the scintillation processes not to be significant for the detector performance. This explains why the energy resolution stabilizes after a certain value of E/p.

While for the shaping constant of 5 μs the signal amplitude results from the total amount of secondary scintillation produced and, therefore, is proportional to the E/p value applied to the region, for a shaping constant of 50 ns the secondary scintillation collected by the PMT has its maximum value for the scintillation produced just above the PMT window, defining the signal amplitude.

In spite of the fact that the mean number of photons produced by the primary electrons is constant in all instants, the number of photons collected by the PMT increases with the approximation of the primary electron cloud to the PMT window, since the solid angle subtended by the PMT increases. This is because the secondary scintillation collected by the PMT is maximum when the first electrons from the primary electron cloud reach the PMT window. In this situation, the average distance from the cloud to the PMT is, in first approximation, equal to the radius of the cloud. Since the diffusion of the cloud, i.e., its length, decreases with E/p, the mean distance from the PMT to the primary electron cloud reduces when E/p increases. The solid angle subtended by the PMT increases also, and the amount of secondary scintillation collected by the PMT adds to the linear increase of the average secondary scintillation produced as a function of E/p. As a result, the signal variation with E/p, for the shaping constant of 50 ns, is faster than the linear variation of the secondary scintillation as function of E/p for 5 μs.

Figure 5 shows the pulse-height distributions from the MCA for 5 μs and 50 ns shaping constants, for a reduced electric field of 4V/cm/torr and PMT bias voltage of 650 V.

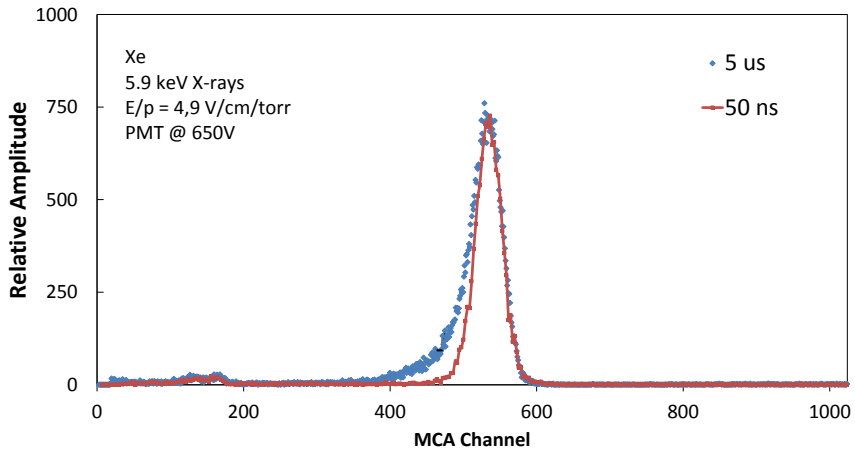

Figure 5: Pulse-height distributions obtained with pure xenon and the getters operating at 150°C for 5 μs and 50 ns shaping constants, for a reduced electric field of 4.9V/cm/torr and a PMT bias voltage of 650 V.

As shown in figure 5, there is a large similarity between the pulse-height distributions for shaping constants of 5 μs and 50 ns. The energy resolution is approximately equal for both cases, but for 50 ns the pulse-height distribution is noticeably better, because it does not present the higher low-energy tail, characteristic of a driftless detector [4, 5].

2.2 Mixtures of xenon and CH_4

In this section we present the results for xenon mixtures with 0.5%, 1.0% and 2.2% of CH_4. A comparison is made with the results for pure xenon.

99.5% Xe + 0.5 % CH_4

Figure 6 shows the variation of the linear dependence of the amplitude on the reduced electric field with time, beginning when 0.5% of CH_4 was added to xenon, with the getters operating at 150ºC. The excitation threshold decreases from 1.76 V/cm/torr, 2.5 hours after adding the CH_4, to 1.46V/cm/torr, 118 hours after adding the CH_4. At 150ºC the getters were absorbing CH_4 and the mixture was not stable. Therefore, in the following studies we reduced the temperature of the getters to 100ºC.

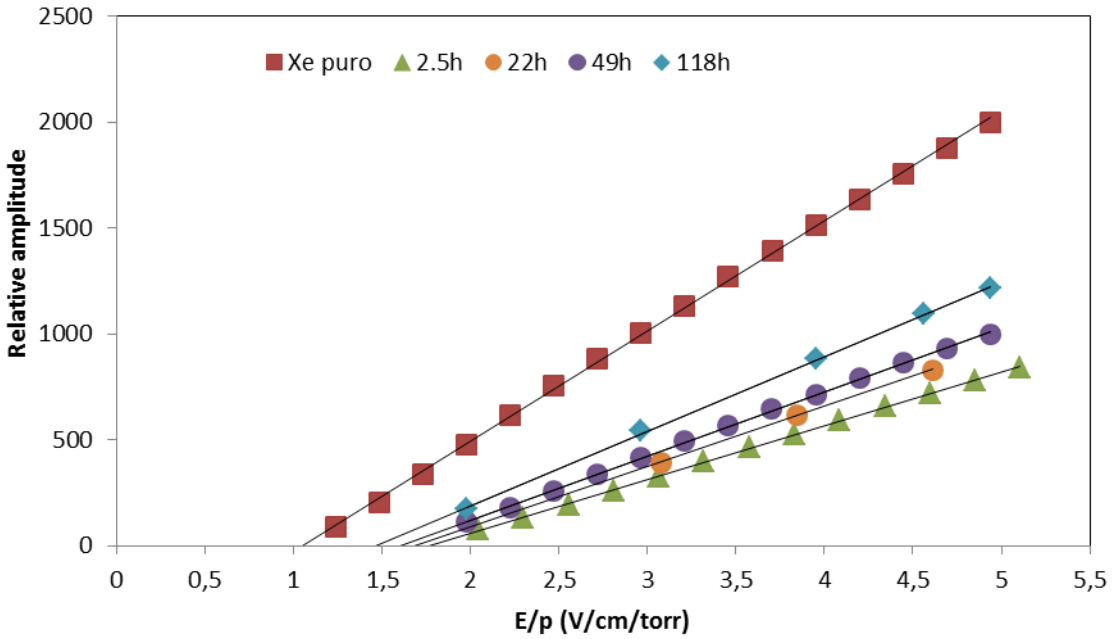

Figure 6: Relative amplitude as a function of reduced electric field, E/p, for the mixture of 99.5% of Xe and 0.5% of CH_4 at 150°C with a filling pressure of 790 torr, for a constant PMT bias voltage of 800 V and a shaping constant of 5 μs.

For the mixture of 99.5% Xe + 0.5% CH4, the excitation threshold was 1.8 V/cm/torr, higher than for pure xenon, as expected. This means that a small percentage of methane added to xenon in the driftless GPSC absorbs the energy that primary electrons gain from the electric field through inelastic collisions, by exciting rotational and vibrational modes. Therefore, a high electric field is needed to produce a certain amount of scintillation.
The energy resolution still decreases with increasing reduced electric field and at 5 V/cm/torr is around 8.4 % FWHM.

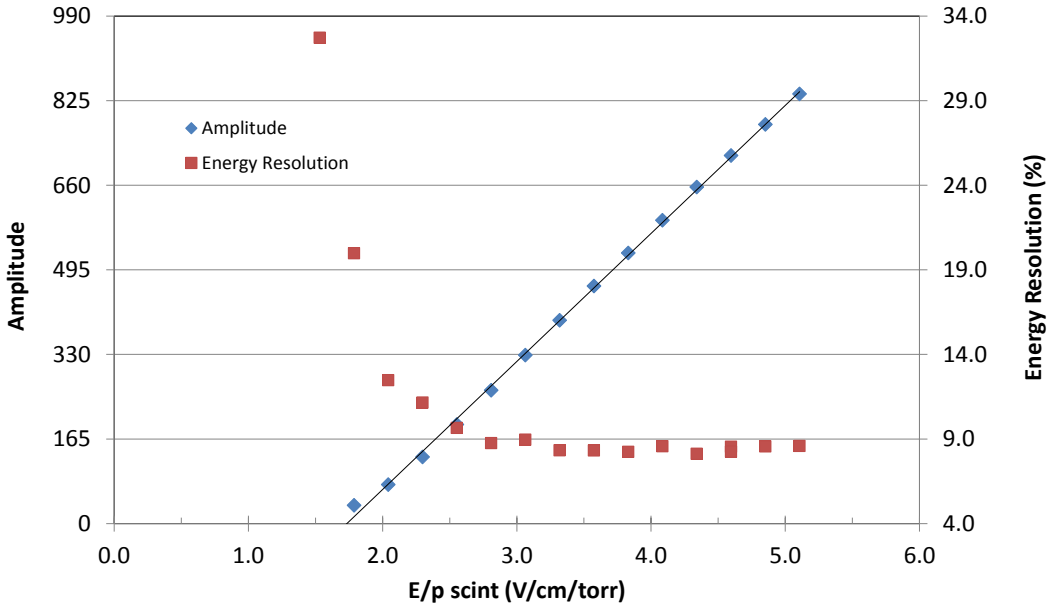

Figure 7: Relative amplitude and energy resolution as a function of reduced electric field, E/p, for the mixture of 99.5% Xe and 0.5% CH_4 at 150°C with a filling pressure of 783 torr, a constant PMT bias voltage of 650 V and formatting constants of 5 μs, 2.5 hour after adding methane to xenon.

99.0% Xe + 1.0 % CH_4

Figure 8 shows amplitude and energy resolution as a function of reduced electric field for the mixture of (99% of Xe and 1% of CH_4) with a gas pressure of 790 torr, for a PMT bias voltage of 800 V and shaping constants of 5 μs.

As shown in figure 8, for this mixture, 99.0%Xe + 1.0%CH_4, the excitation threshold is 2.33 V/cm/torr, and is higher than the one for pure xenon and also higher than the one for the mixture 99.5% Xe + 0.5 % CH_4, as expected.

The energy resolution at 5 V/cm/torr is around 9.2 % FWHM, still decreasing with increasing reduced electric field.

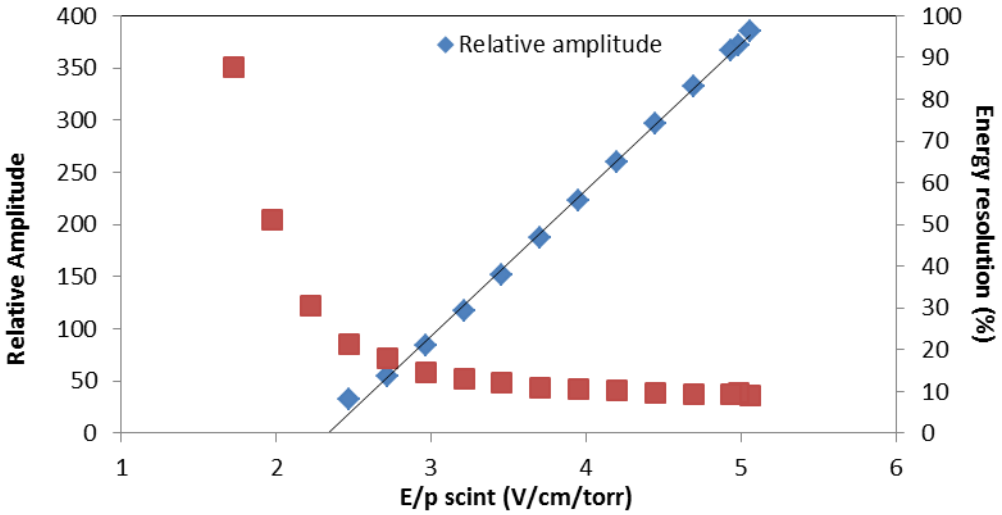

Figure 8: Amplitude and energy resolution as a function of reduced electric field, E/p for the mixture of 99% of Xe and 1% of CH_4 at 100°C, with a filling pressure of 790 torr, a constant PMT bias voltage of 800 V and formatting constant of 5 μs.

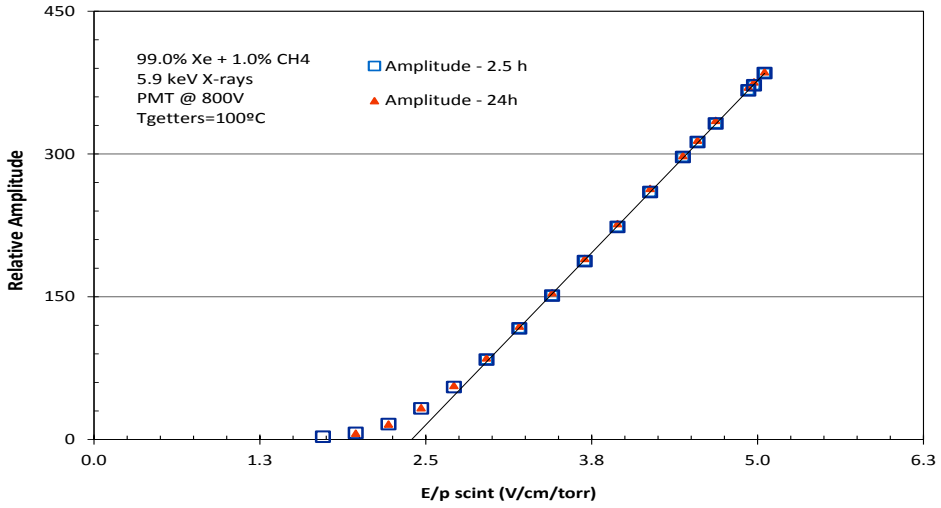

Figure 9: Relative amplitude as a function of reduced electric field, E/p, for the mixture of 99.0% Xe + 1.0 % CH_4 at 100°C, with a filling pressure of 792 torr, for a constant PMT bias voltage of 800 V and shaping constants of 5 μs.

Figure 9 shows the variation of the linear dependence of the amplitude on the reduced electric field with time. The figure shows the results for the time stamps 2.5 hours after the addition of 1.0% of CH_4 to xenon (stable),) and 24 hours later. At 100ºC the getters didn't seem to absorb the CH_4 and, therefore, the mixture was stable. The operating temperature of the getters was set to 100ºC when operating with mixtures of CH_4 and xenon.

97.8% Xe + 2.2 % CH_4

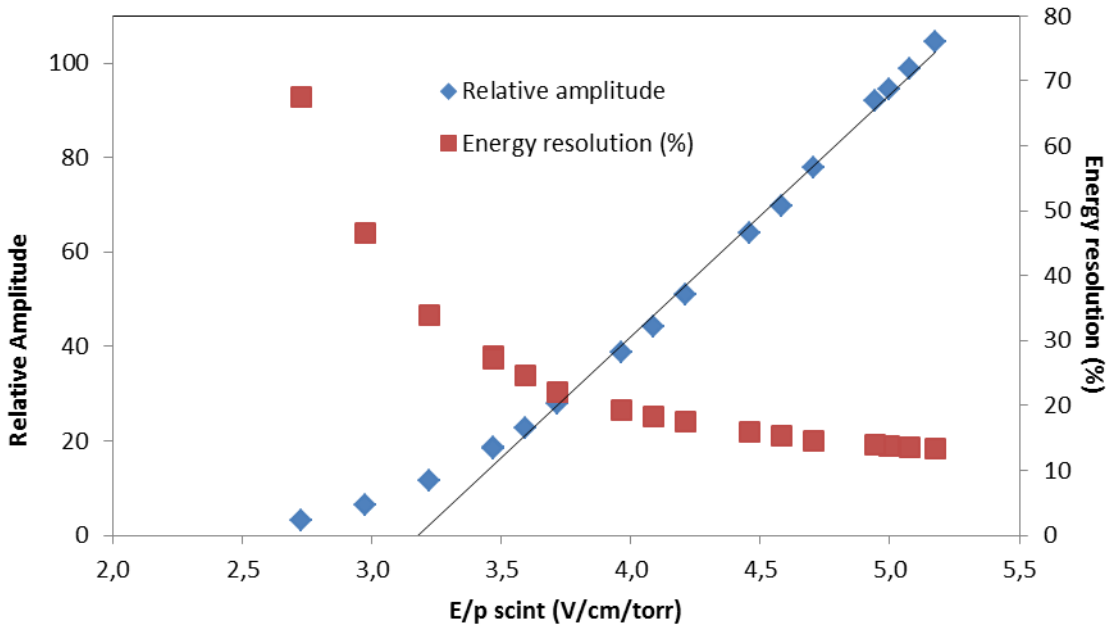

Figure 10: Amplitude and energy resolution as a function of reduced electric field, E/p, for the mixture of 97.8% of Xe and 2.2% of CH_4 at 100°C with a filling pressure of 776 torr, a constant PMT bias voltage of 800 V and formatting constants of 5 μs.

For the mixture 97.8 % Xe + 2.2% CH4, the excitation threshold was 3.18 V/cm/torr. Energy resolution was about 13% for an E/p close to 5 V/cm/torr.

2.3 Energy Resolution

A comparison of the energy resolution as a function of reduced electric field, for xenon and xenon-methane mixtures is shown in Figure 11.

As seen in figure 11, the higher the percentage of methane added to xenon, the higher the energy resolution. For instance, for an E/p of 3.5 V/cm/torr, the energy resolution has values of 8.1%, 8.3% and 12% for pure xenon, 99.5%Xe + 0.5%CH4 and 99.0%Xe + 1.0%CH4, respectively. However, operating at higher reduced electric fields in the scintillation region will improve the energy resolution to values close to the values obtained for pure xenon, as will be discussed ahead.

We need to extrapolate the energy resolutions obtained in this work to $Q_{\beta\beta}$, but at 1 bar, we obtain the values presented in tables 1 and 2. We considered E/p values of 3.5 and 4.7 V/cm/torr because NEXT-TPC will operate in this range of scintillation reduced electric field.

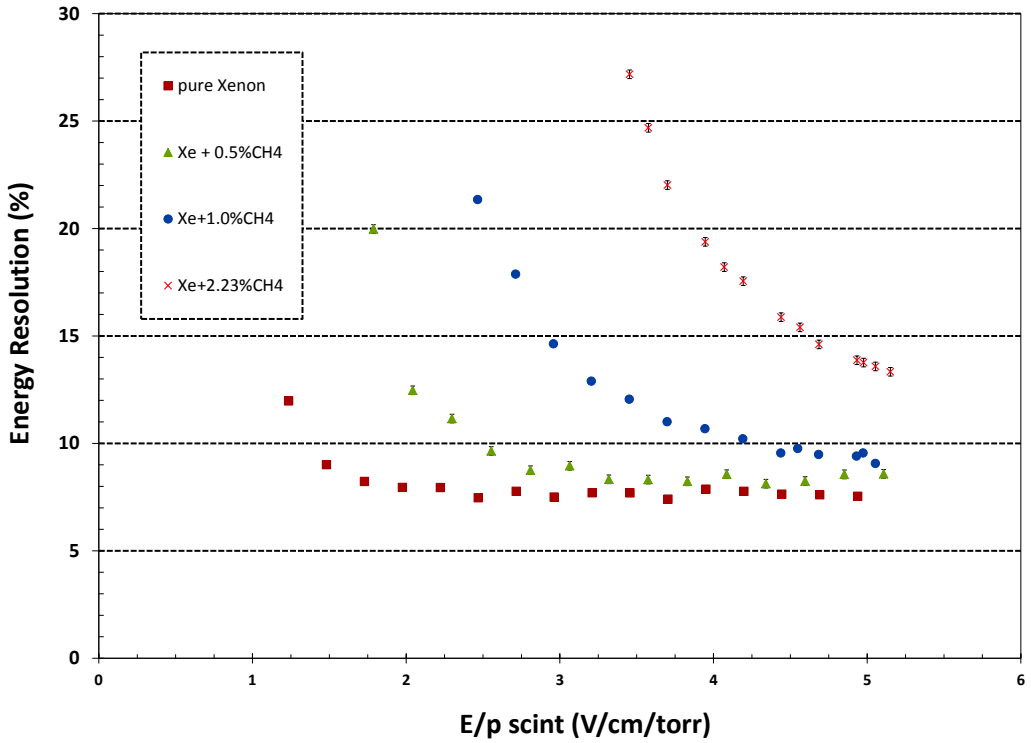

Figure 11: Energy resolution as a function of reduced electric field in the scintillation region, E/p_{scint} for pure xenon and xenon-methane mixtures.

Table 1: Extrapolation of energy resolution, ER, for 2.5 MeV for an applied E/p of 3 V/cm/torr at 1 bar and the voltage applied to the drift and scintillation regions of NEX-TPC.

E/p (V/cm/torr) =	3.5			0.15
	ER(%) for 5.9 keV	ER(%) for 2458 keV	HV (kV) Scint. region	HV (kV) Drift region
Xe	7,7	0,38	7.98 @ 10 bar 11.97 @ 15 bar	114 @10 bar 171 @15 bar
$Xe+0.5\%CH_4$	8,3	0,41		
$Xe+1.0\%CH_4$	12,0	0,59		
$Xe+2.2\%CH_4$	27,0	1,32		

Table 2: Extrapolation of energy resolution, ER, for 2.5 MeV for an applied E/p of 4.7 V/cm/torr at 1 bar and the voltage applied to the drift and scintillation regions of NEX-TPC.

E/p (V/cm/torr) =	4.7			0.15
	ER (%) for 5.9 keV	ER(%) for 2458 keV	HV (kV) Scint. region	HV (kV) Drift region
Xe	7,61	0,37	10.72 @10bar 16.07 @15bar	114 @10 bar 171 @15 bar
$Xe+0.5\%CH_4$	8,45	0,41		
$Xe+1.0\%CH_4$	9,5	0,47		
$Xe+2.2\%CH_4$	14,6	0,72		

2.4 Electron Drift Velocity

In this section we compared Monte Carlo simulations with experimental results for pure and doped xenon. The results were obtained from the time duration of the scintillation pulses, obtained using the 50 ns shaping constants, for 2.5 cm drift path of the primary electron cloud.

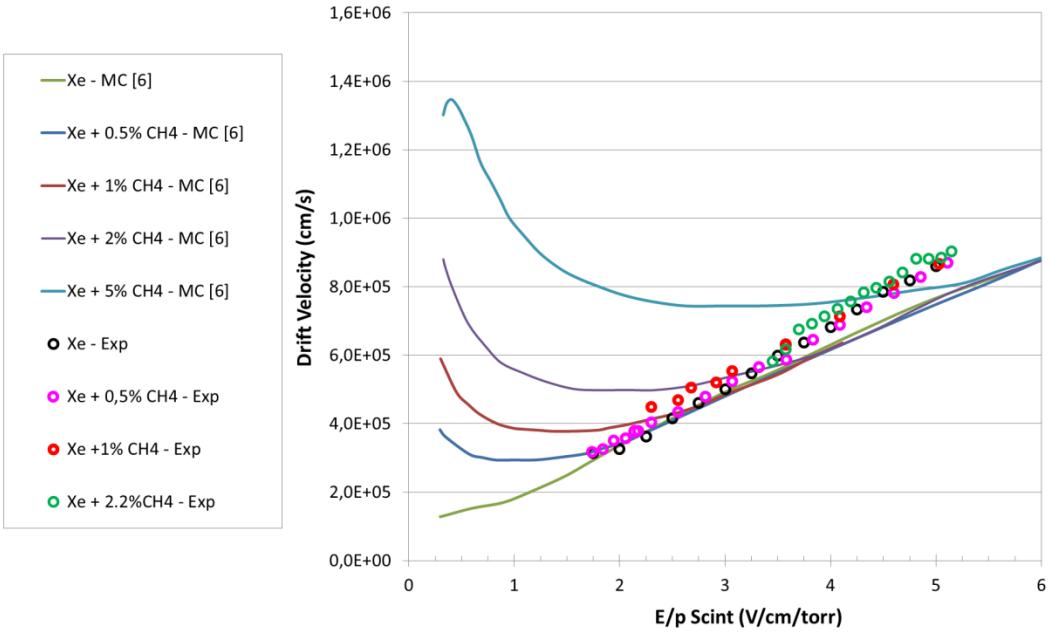

Figure 12: Comparison of electron drift velocity as function of E/p for Monte Carlo simulations (lines) [6] and our experimental results (symbols).

Figure 12 presents all of our experimental electron drift velocity results which are compared to Monte Carlo (MC) simulations [6]. The results obtained are in good agreement with those obtained with MC simulations and with other experimental results.

2.5 Electroluminescence yield

We calculated the reduced EL yield for different values of the reduced electric field, for Xe+CH_4 mixtures.

Figure 13 presents the reduced EL yield, Y/N, i.e. the EL yield divided by the density of the gas, as a function of reduced electric field, E/p, in the scintillation region of the driftless GPSC. Experimental results from other authors and results from Monte Carlo simulations [6] are included for comparison.

The results obtained in this work were relative amplitudes. Absolute values were obtained normalizing the relative values of pure xenon to the absolute values of Monteiro et al. [9] for pure xenon.

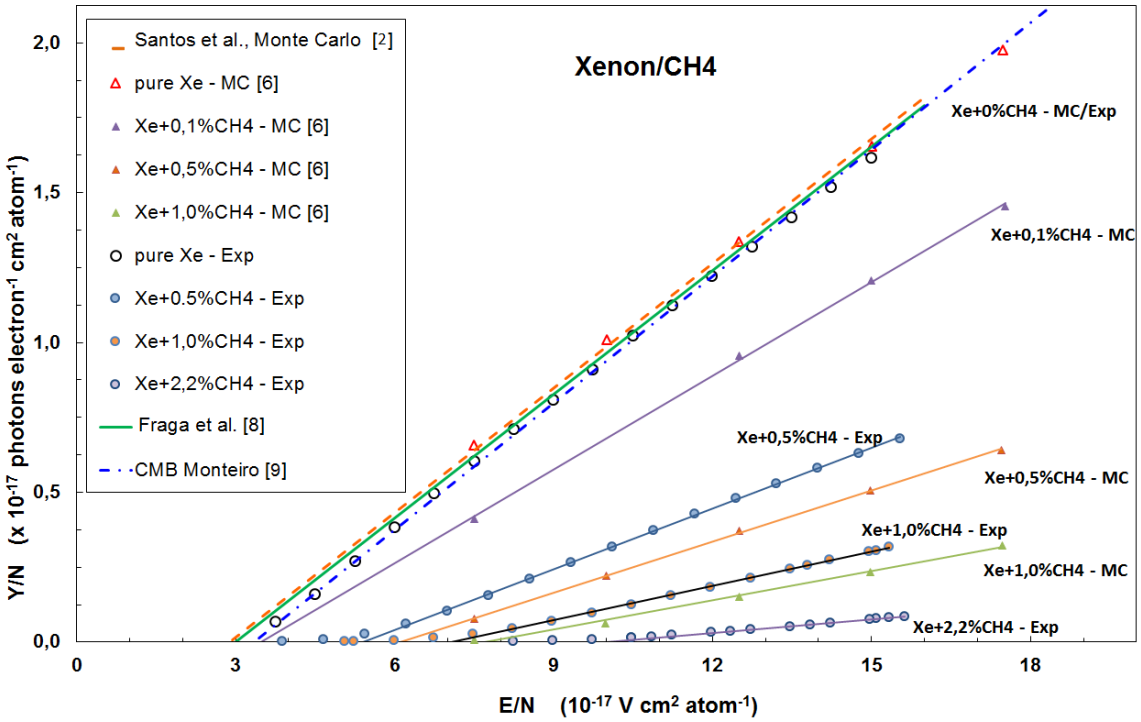

Figure 13: Xenon reduced electroluminescence yield as a function of reduced electric field for our studies, as well as for the different data reported in the literature.

Tables 3 and 4 present the dependencies between Y/N and E/N or E/p for the mixtures 99.5%Xe + 0.5%CH_4 and 99.0% Xe +1.0% CH_4, respectively, and from Monte Carlo simulation results for the same mixtures.

Table 3: Scintillation amplification parameter for the mixture (99.5% Xe and 0.5% CH4), reduced electroluminescence yield linear trends at 20°C for the present studies, as well as for Monte Carlo simulation results [6].

Work	Amplification parameter (photon/kV)	Linear Trend Density units*
Our work	68	Y/N = 0.068 E/N- 0.366
MC Escada	57	Y/N = 0,057E/N – 0.348

* *E/N* in Td (10^{-17} V cm^2 $atom^{-1}$)

Table 4: Scintillation amplification parameter for the mixture (99% Xe and 1% CH4), reduced electroluminescence yield linear trends at 20°C for the present studies, as well as for Monte Carlo simulation results [6].

Work	Amplification parameter (photon/kV)	Linear Trend Density units*
Our work	38	Y/N = 0.038 E/N – 0.269
MC Escada	32	Y/N = 0.032 E/N – 0.248

* *E/N* in Td (10^{-17} V cm^2 atom^{-1})

For the mixture of 97.8% xenon and 2.2% CH_4, the variation of the reduced electroluminescence yield with reduced electric field in temperature independent units can be approximately represented by

$$Y/N\ (10^{-17} photons\ electron^{-1} cm^2 atom^{-1} = 0.0149 \frac{E}{N} - 0.1479$$

where E/N is given in Td (10^{-17} V cm^2 atom^{-1}).

And the amplification parameter for the mixture (97.8% Xe and 2.2% CH_4) is 14.9 photons/kV.

As shown, the amplification parameters for the mixtures (99.5% Xe and 0.5% CH4) and (99% Xe and 1% CH4) are not very different from those predicted by Monte Carlo simulation for the same mixtures. Compared to pure xenon, the EL yield decreases to 50% for 0.5% of CH_4, to 30% for 1% of CH_4 and to 10% for 2.2% of CH_4. This proves that the amount of secondary scintillation in noble gases decreases with increasing impurity content.

2.6 F*w* and Intrinsic Resolution

The Fano factor denotes the relative variance of the distribution, and its value ranges between 0 and 1. Higher values of the Fano factor indicate a broader distribution of the number of electron-ion pairs than that described by lower values of *F*. The *W* and *F* values are characteristics of a gas, they only slightly depend on the kind of the incident particle; and both increase (w towards infinity, *F* towards 1) as the initial electron energy decreases approaching the ionization potential of a gas.

The energy resolution can be given by:

$$R = 2{,}355\sqrt{\frac{Fw}{E_x} + \frac{2}{N_e}}$$

$$R^2 = 5{,}546\left(\frac{Fw}{E_x} + \frac{k}{A}\right)$$

where A is proportional to the centroid channel, of the Gaussian fitted to the spectrum main peak. Plotting R^2 versus the reciprocal of the pulse amplitude A, 1/A, the extrapolation to infinite amplitudes (i.e. 1/A->0) gives the square of the intrinsic energy resolution, R_{int}. The Fano factor can be obtained if E and *w* are known.

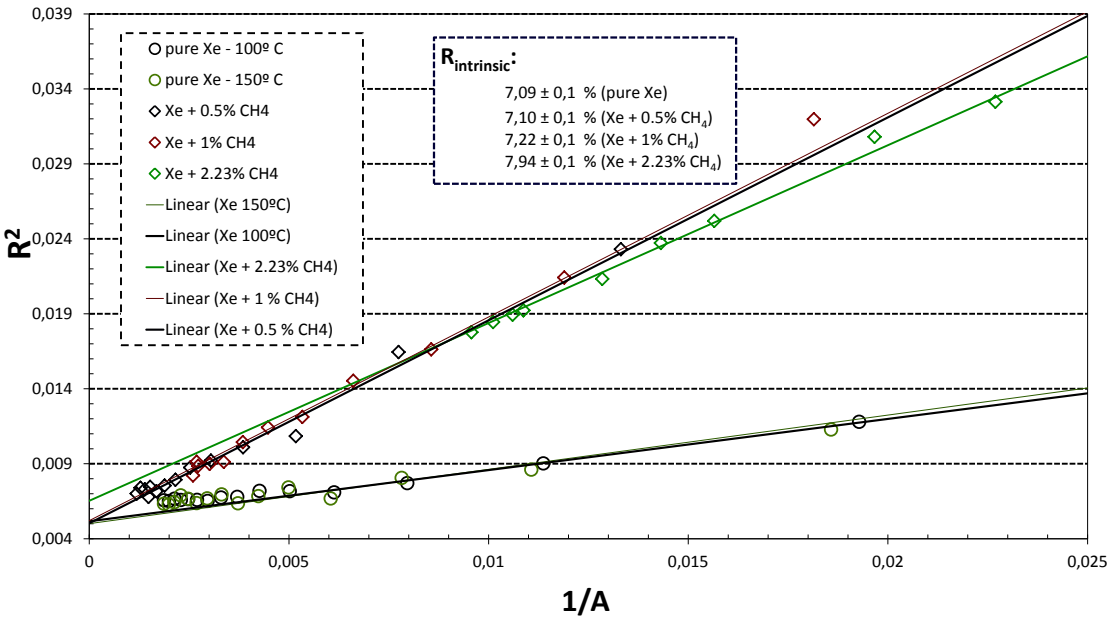

Figure 14: Dependence of R^2 on the inverse of the pulse amplitude, A, with the extrapolation to infinite amplitudes for pure xenon and Xe-CH_4 mixtures, used in this work.

With the obtained experimental results (see figure 14), we were able to determine the intrinsic energy resolution and the value of F*w*, for each mixture, see Table5.

Table 5: Experimental results obtained for Fw and R_{int} for pure xenon and for different Xe-CH_4 mixtures.

Gas Mixture	F*w* (eV)	R_{int}(%)
Pure Xe	5.34	7.09±0.1
Xe + 0.5% CH4	5.35	7.10±0.1
Xe + 1.0% CH4	5.54	7.22±0.1
Xe + 2.2% CH4	6.70	7.94±0.1

3. Conclusions

Since the early development of GPSCs with uniform field geometries, the approximately linear dependence of the reduced EL yield on the reduced electric field in the scintillation region is well stablished and known. The scintillation threshold corresponds to a reduced electric field of about 0.8 kV/cm/bar (or 1.0 V/cm/torr) [1] for pure xenon.

However, for xenon-CH_4 mixtures, the amplification parameter (the number of photons produced per drifting electron and per volt – the slope of the linear dependence referred to

above) had not been established in the literature yet, presenting only values from one Monte Carlo simulation model [2]. In the experimental work described in this report, this parameter was measured and was found to decrease for these mixtures; the higher the percentage of the impurity, the smaller the amplification parameter, in agreement with the Monte Carlo results.

The scintillation amplification parameter for pure xenon was used as reference to obtain the relative EL yields of 68 photons/kV for xenon with 0.5% of CH_4, 38 photons/kV for 1% of CH_4 and 15 photons/kV for 2.2% of CH_4. This compares with the Monte Carlo values of 57 and 32 photons/kV for Xe+0.5% CH_4 and Xe+1.0% CH_4, respectively. This reduction in EL has to be taken into account if the addition of CH_4 to xenon is to be considered. A compromise between the mixture EL yield and electron diffusion has to be found.

Comparing with Monte Carlo simulations results of the EL yield, we had 19% more of EL in this work than in simulations by Escada et al. [2]. We know that these simulations considered ideal conditions and did not take into account all the effects that occur in the detector.

The results of electron drift velocity for pure xenon and mixtures are in good agreement with those obtained with Monte Carlo simulations, as shown in figure 12.

For the NEXT experiment, the energy resolution parameter is more important than the EL yield, which can be more than what is needed for optimum energy resolution. The energy resolution in NEXT should be as close to the intrinsic value as possible, i.e. the lowest achievable for a GPSC.

Our studies have shown that the 99.5%Xe + 0.5%CH_4, 99.0%Xe + 1.0%CH_4 mixtures are adequate for using in NEXT, since the intrinsic energy resolution degradation is negligible, while the drift velocity of the primary electron cloud increases ~5 and ~7 fold for 0.5 and 1.0% of CH_4 content respectively, when compared to pure Xe, at E/p ~0.15 V/cm/torr.

References

[1] P.C.P.S. Simões, D.S. Covita, J.F.C.A. Veloso et al., *A new method for pulse analysis of driftless-gas proportional scintillation counters*, Nuclear Instruments and Methods in Physics Research A 505:1-2 (2003) 247

[2] F P Santos, T H V Dias, A D Stauffer and C A N Conde, *Three – dimensional Monte Carlo calculation of the VUV electroluminescence and other electron transport parameters in xenon*, J. Phys. D: Appl. Phys. 27 (1994) 42

[3] D.G. Simons and P.A.J. De Korte, *Soft X-ray energy resolution and background rejection in driftless gas scintillation counter*, Nucl. Instr. And Meth. A277 (1989) 642

[4] P.C.P.S. Simões, J. M. F. dos Santos and C. A. N. Conde, *Driftless gas proportional scintillation counter pulse analysis using digital processing techniques*, X-Ray Spectrometry 30 (2001) 342

[5] D.S. Covita, P.C.P.S. Simões, L.M.P. Fernandes, *The X-ray performance of a driftless gas proportional scintillation counter using short shaping-time constants for pulse analysis*, Nuclear Instruments and Methods in Physics Research A 516 (2004) 134

[6] J. Escada, T.H.V.T. Dias, F.P. Santos et al, *A Monte Carlo study of the fluctuations in Xe electroluminescence yield: pure Xe vs Xe doped with CH4 or CF4 and planar vs cylindrical geometries*, JINST 6 (2011) P08006

[7] Hiroki Kusano, José A. Matias-Lopes, Mitsuhiro Miyajima et al., *Electron Mobility and Longitudinal Diffusion Coefficient in High-Density Gaseous xenon*, Japanese Journal of Applied Physics 51 (2012) 116301

[8] M M F R Fraga, C M Ferreira, J Loureiro and MS Leite, P 1990 ESCAMPIG (Orleans, France, 28-31 Aug)

[9] C. M .B. Monteiro, L. M. P. Fernandes, J. A. M. Lopes, et al., *Secondary scintillation yield in pure xenon*, JINST 2 (2007) P05001.